

# Chapter 3

## Physical Environment



Chapter 1  
Introduction and  
Background

Chapter 2  
Management  
Direction

Chapter 3  
Physical  
Environment

Chapter 4  
Biological  
Environment

Chapter 5  
Human  
Environment

Appendices



## Chapter 3. Physical Environment

### 3.1 Climate and Climate Change

#### 3.1.1 General Climate Conditions

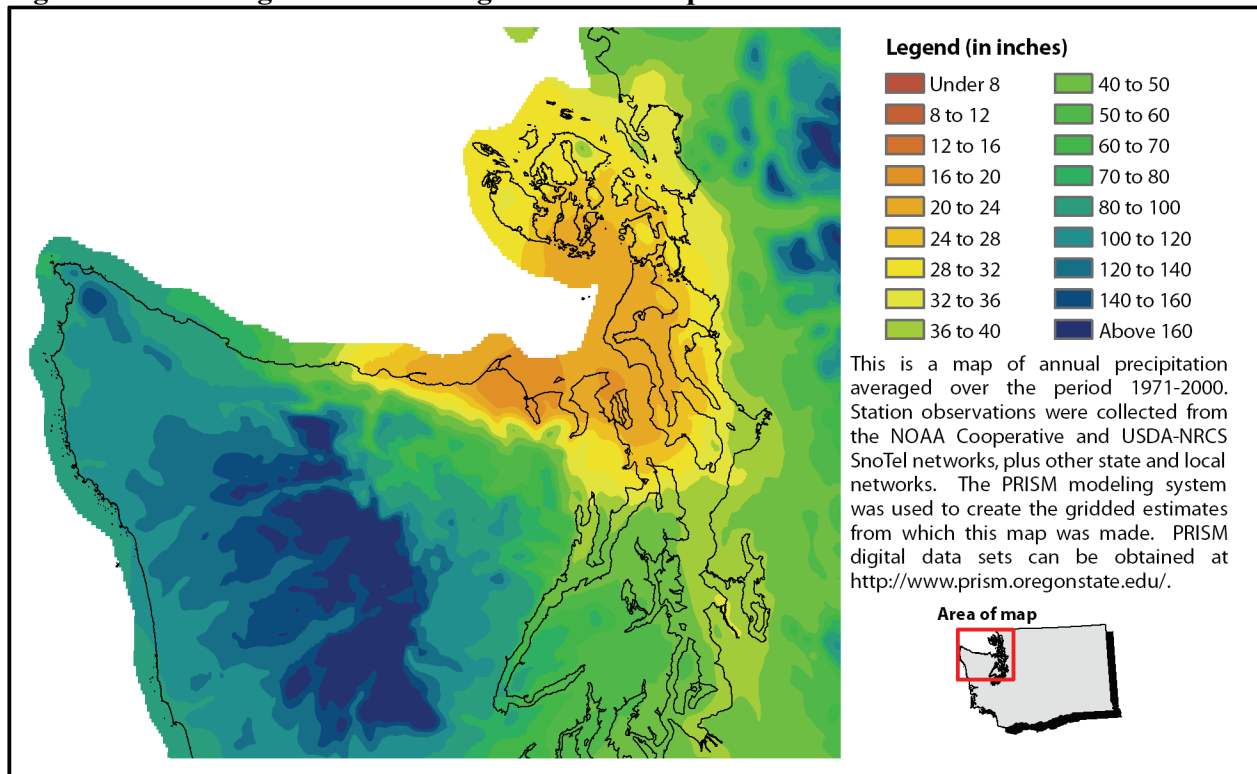
The climate at Dungeness National Wildlife Refuge (NWR) is a mild, midlatitude west coast marine type. Because of the moderating influence of the Pacific Ocean, extremely high or low temperatures are rare. Summers are generally cool and dry while winters are mild but moist and cloudy with most of the precipitation falling between November and January (USDA 1987, WRCC 2011a). Annual precipitation in the region is low due to the rain shadow cast by the Olympic Mountains and the extension of the Coastal Range on Vancouver Island (Figure 3-1). Snowfall is rare or light. During the latter half of the summer and in the early fall, fog banks from over the ocean and the Strait of Juan de Fuca cause considerable fog and morning cloudiness (WRCC 2011a).

#### Climate Change Trends

The greenhouse effect is a natural phenomenon that assists in regulating and warming the temperature of our planet. Just as a glass ceiling traps heat inside a greenhouse, certain gases in the atmosphere, called greenhouse gases (GHG), absorb and emit infrared radiation from sunlight. The primary greenhouse gases occurring in the atmosphere include carbon dioxide (CO<sub>2</sub>), water vapor, methane, and nitrous oxide. CO<sub>2</sub> is produced in the largest quantities, accounting for more than half of the current impact on the Earth's climate.

A growing body of scientific evidence has emerged to support the fact that the Earth's climate has been rapidly changing and the magnitude of these alterations is largely due to human activities (IPCC 2007a, NAS 2008, USGCRP 2009). Although climate variations are well documented in the Earth's history, even in relatively recent geologic time (e.g., the Ice Age of approximately 10,000 years ago), the current warming trend differs from shifts earlier in geologic time in two ways. First, this climate change appears to be driven primarily by human activities such as deforestation and the burning of fossil fuels which results in a higher concentration of atmospheric GHG. Second, atmospheric CO<sub>2</sub> and other greenhouse gases, levels of which are strongly correlated with the Earth's temperature, are now higher than at any time during the last 800,000 years (USGCRP 2009). Prior to the start of the Industrial Revolution in 1750, the amount of CO<sub>2</sub> in the atmosphere was about 280 parts per million (ppm). Current levels are about 390 ppm and are increasing at a rate of about 2 ppm/year (DOE 2012). The current concentration of CO<sub>2</sub> and other greenhouse gases as well as the rapid rate of increase in recent decades are unprecedented in the prehistoric record (Ibid).

The terms "climate" and "climate change" are defined by the Intergovernmental Panel on Climate Change (IPCC). The term "climate" refers to the mean and variability of different types of weather conditions over time, with 30 years being a typical period for such measurements, although shorter or longer periods also may be used (IPCC 2007b). The term "climate change" thus refers to a change in the mean or variability of one or more measures of climate (e.g., temperature or precipitation) that persists for an extended period, typically decades or longer, whether the change is due to natural variability, human activity, or both (Ibid).

**Figure 3-1. Washington State Average Annual Precipitation from 1971 to 2000**

Scientific measurements spanning several decades demonstrate that changes in climate are occurring, and that the rate of change has been faster since the 1950s (Figure 3-2). Examples include warming of the global climate system, and substantial increases in precipitation in some regions of the world and decreases in other regions (e.g., IPCC 2007b, Solomon et al. 2007). In the Pacific Northwest, increased greenhouse gases and warmer temperatures have resulted in a number of physical and chemical impacts. These include changes in snowpack, stream flow timing and volume, flooding and landslides, sea levels, ocean temperatures and acidity, and disturbance regimes such as wildfires, insect, and disease outbreaks (USGCRP 2009). All of these changes will cause major perturbations to ecosystem conditions, possibly imperiling species that evolved in response to local conditions.

Results of scientific analyses presented by the IPCC show that most of the observed increase in global average temperature since the mid-20th century cannot be explained by natural variability in climate, and is “very likely” (defined by the IPCC as 90 percent or higher probability) due to the observed increase in greenhouse gas (GHG) concentrations in the atmosphere as a result of human activities, particularly carbon dioxide emissions from use of fossil fuels (IPCC 2007b, Solomon et al. 2007). Further confirmation of the role of GHGs comes from analyses by Huber and Knutti (2011), who concluded that it is extremely likely that approximately 75 percent of global warming since 1950 has been caused by human activities.

In the Northern Hemisphere, recent decades appear to be the warmest since at least about A.D. 1000, and the warming since the late 19th century is unprecedented over the last 1,000 years. Globally, including 2011, the first 11 years in the 21<sup>st</sup> century (2001 to 2011) rank among the 13 warmest years in the 130-year instrumental record (1880 to present) according to independent analyses by NOAA and NASA. 2010 and 2005 are tied as the warmest years in the instrumental record and the new 2010 record is particularly noteworthy because it occurred in the presence of a La Niña and a period of low

solar activity, two factors that have a cooling influence on the planet. However, in general, decadal trends are far more important than any particular year's ranking.

Trends in global precipitation are more difficult to detect than changes in temperature because precipitation is generally more variable and subject to local topography. However, while there is not an overall trend in precipitation for the globe, significant changes at regional scales can be found. Over the last century, there have been increases in annual precipitation in the higher latitudes of both hemispheres and decreases in the tropical regions of Africa and southern Asia (USGCRP 2009). Most of the increases have occurred in the first half of the 20th century and it is not clear that this trend is due to increasing greenhouse gas concentrations.

Just as important as precipitation totals are changes in the intensity, frequency, and type of precipitation. Warmer climates, owing to increased water vapor, lead to more intense precipitation events, including more snowstorms and possibly more flooding, even with no change in total precipitation (Dominguez et al. 2012).

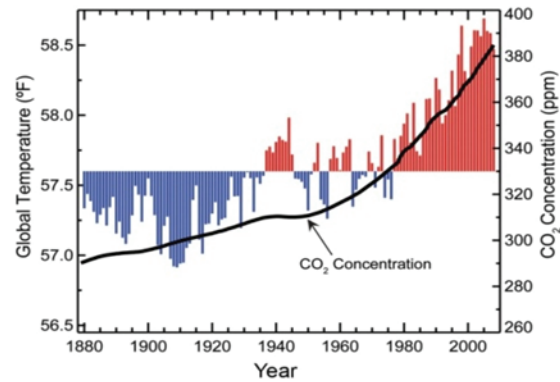
The frequency of extreme single-day precipitation events has increased, especially in the last two decades. Paradoxically more droughts and heat waves have occurred because of hotter, longer-lasting high pressure systems.

### 3.1.2 Air Temperatures

There is no climate/weather station established on Dungeness NWR; however, temperature data have been consistently collected since October 1980 at the Sequim 2 E station (number 457544) located approximately 7 miles east of the Refuge. The proximity of this station to the Refuge provides valuable regional data. Table 3-1 provides a summary of the period of record.

As a result of the ocean's proximity, winter minimum and summer maximum temperatures are moderated. On average, 91.7 days per year experience minimum temperatures at or below freezing while 0.1 days per year experience temperatures at or below 0°F (WRCC 2011b). The coldest weather is usually associated with an outbreak of cold air from the interior of Canada. The first occurrence of freezing temperatures is usually in October (WRCC 2011c). The date of the last freezing temperatures in the spring ranges from the latter half of April to the first half of May (WRCC 2011d). Also, it is only in the extreme occurrences that temperatures have been recorded to exceed 90°F (WRCC 2011b).

**Figure 3-2. Global Annual Average Temperature and CO<sub>2</sub> from 1880-2008 (NOAA 2012a)**



Global annual average temperature (as measured over both land and oceans). Red bars indicate temperatures above and blue bars indicate temperatures below the average temperature for the period 1901-2000. The black line shows atmospheric carbon dioxide (CO<sub>2</sub>) concentration in parts per million (ppm). While there is a clear long-term global warming trend, each individual year does not show a temperature increase relative to the previous year, and some years show greater changes than others.<sup>33</sup> These year-to-year fluctuations in temperature are due to natural processes, such as the effects of El Niños, La Niñas, and the eruption of large volcanoes.

**Table 3-1. Air Temperature Summary near Dungeness NWR (WRCC 2011b)**

Temperatures (°F)	Sequim 2 E Oct. 1980 – Dec. 2010
Average Monthly Temperature – High	57.6
Average Monthly Temperature – Low	39.3
Monthly Mean Winter Temperature – High	47.0
Monthly Mean Winter Temperature – Low	31.2
Monthly Mean Summer Temperature – High	68.6
Monthly Mean Summer Temperature – Low	49.0
Daily Maximum Extreme – High	94
Daily Maximum Extreme – Low	63
Daily Minimum Extreme – High	39
Daily Minimum Extreme – Low	-3

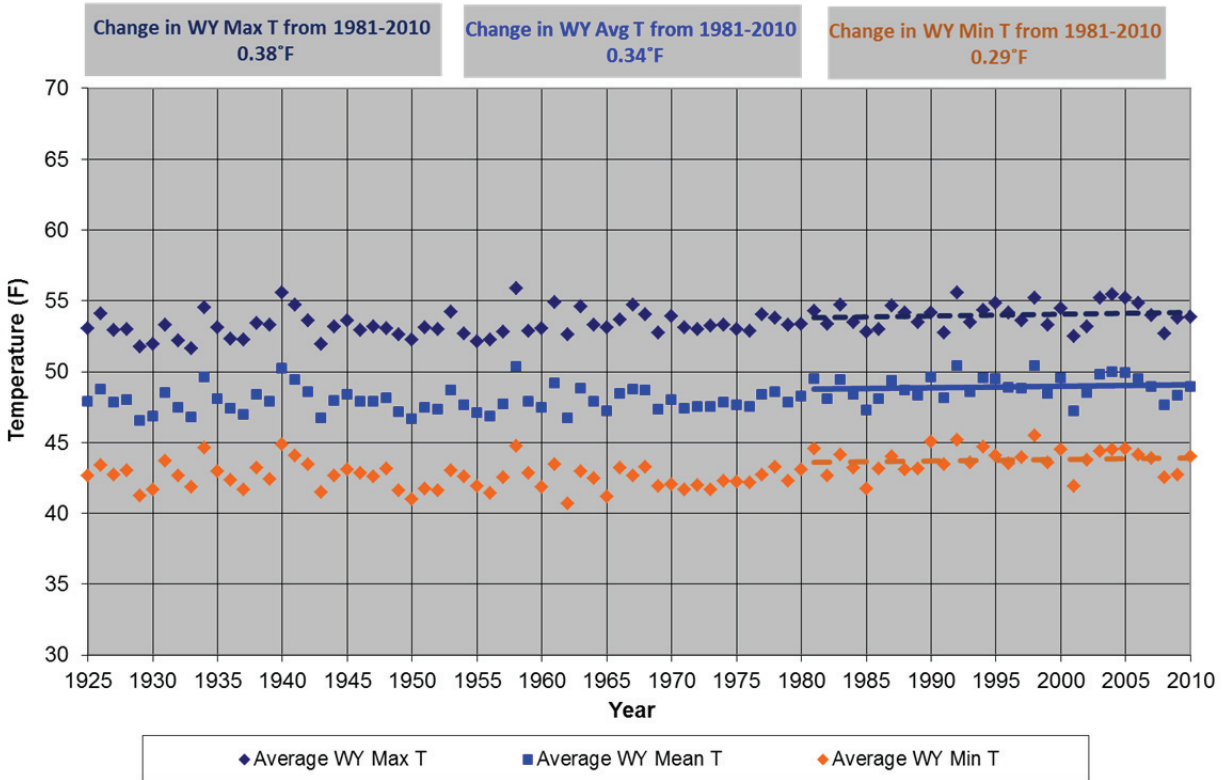
Mote (2003) observed that the Pacific Northwest region experienced warming of approximately 1.5°F during the 20th century. Fu et al. (2010) found that in Washington State from 1952 to 2002, annual mean air temperature increased 1.1°F (daily mean), 0.43°F (daily maximum), and 1.67°F (daily minimum), on average. For trends local to the Refuge we turn to the United States Historical Climatology Network (USHCN) which provides a high quality data set of daily and monthly records of basic meteorological variables from 1,218 observing stations throughout the continental U.S. The data have been corrected to remove biases or heterogeneities from nonclimatic effects such as urbanization or other landscape changes, station moves, and instrument and time of observation changes. The closest station is Port Angeles and trends are provided in Table 3-2 and Figure 3-3. The average yearly temperature change has increased 0.34°F over the past 30 years, and more striking are the seasonal trends which show warmer winters, summers, and falls than the yearly trends, and cooler springs (Table 3-2).

**Table 3-2. Seasonal Temperature Trends, 1981-2010 (USHCN 2012)**

Port Angeles, WA United States Historical Climatology Network Observation Station			
Monthly Absolute Change	Maximum Temp.	Average Temp.	Min. Temp.
Winter (Dec-Feb)	+1.36°F	+0.63°F	-0.11°F
Spring (March-May)	-0.60°F	-0.48°F	-0.36°F
Summer (Jun-Aug)	+0.46°F	+0.69°F	+0.93°F
Fall (Sept-Nov)	+0.36°F	+0.56°F	+0.77°F

The graph below illustrates a sample of these temperature trends using monthly data. The most recent 30-year period is calculated using the slope of the linear trend line, and temperature change is shown as an absolute change over the 30-year period. A water year is defined as the 12-month period from October 1, for any given year, through September 30 of the following year. The water year is designated by the calendar year in which it ends and which includes 9 of the 12 months.

**Figure 3-3. Water Year Temperature 1925-2010 at Port Angeles, WA (USHCN 2012)**



### Future Trends

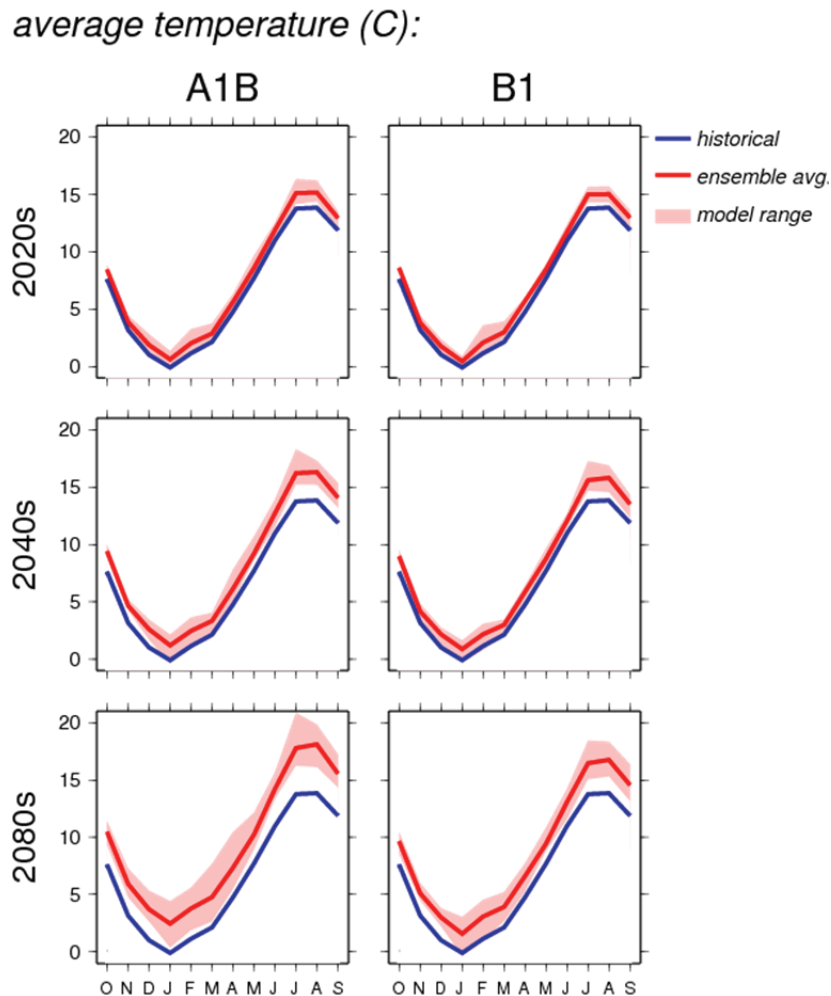
Scientists use a variety of climate models, which include consideration of natural processes and variability, as well as various scenarios of potential levels and timing of GHG emissions, to evaluate the causes of changes already observed and to project future changes in temperature and other climate conditions (Meehl et al. 2007, Ganguly et al. 2009, Prinn et al. 2011). All combinations of models and emissions scenarios yield very similar projections of increases in the most common measure of climate change, average global surface temperature (commonly known as global warming), until about 2030. Although projections of the magnitude and rate of warming differ after about 2030, the overall trajectory of all the projections is one of increased global warming through the end of this century, even for the projections based on scenarios that assume that GHG emissions will stabilize or decline. Thus, there is strong scientific support for projections that warming will continue through the 21st century, and that the magnitude and rate of change will be influenced substantially by the extent of GHG emissions (IPCC 2007c, Meehl et al. 2007, Ganguly et al. 2009, Prinn et al. 2011).

The statistical downscaling of an ensemble of 20 global climate models and two carbon emissions scenarios for each model run projects average annual temperature for the Pacific Northwest to increase 2.0°F (1.1°C) by the 2020s, 3.2°F (1.8°C) by the 2040s, and 5.3°F (3.0°C) by the 2080s, relative to the 1970-1999 average temperature (Mote and Salathé 2009, 2010). The projected changes in average annual temperature are substantially greater than the 1.5°F (0.8°C) increase in average annual temperature observed in the Pacific Northwest during the 20th century. Seasonally, summer temperatures are projected to increase the most. The emissions scenarios modeled included the A1B scenario, which assumes moderate greenhouse gas emissions in the future, and the B2 scenario, which assumes low greenhouse gas emissions in the future. Actual global emissions of greenhouse

gases in the past decade have so far exceeded even the highest IPCC emissions scenario (A2), which was not included in Mote and Salathé (2009, 2010) or Salathé et al. (2010). Consequently, if these emissions trends continue the climate projections referenced herein likely represent a conservative estimate of future climatic changes.

The two regional climate simulations (Salathé et al. 2010) using a dynamical downscaling method with two global climate models (the CCSM3 and ECHAM5 – to specify boundary climate conditions within the region) support the warming increases described above, with small variations – one model slightly higher and one slightly lower. Both regional climate models project increases in heat wave frequency and the frequency of warm nights throughout the State of Washington. Figure 3-4 shows these modeled, downscaled temperature projections for the Dungeness-Elwha watershed (HUC 17110020) (Hamlet et al. 2010).

**Figure 3-4. Projected Temperature Changes for the Dungeness-Elwha Watershed under Two Emission Scenarios (Hamlet et al. 2010)**



Note: A1B is a higher emission scenario than B1. Current rates are higher than both A1B and B1.

### 3.1.3 Precipitation

The prevailing wind direction across the Olympic Peninsula from the southwest, means that storms frequently drop their moisture on the west side of the Olympic Mountains. Consequently, the relatively low precipitation at Dungeness NWR is the result of its location in the “rain shadow.” The rain shadow is an area that extends east from Port Angeles towards Everett and north into the San Juan Islands (Bach 2004).

The discussion below includes data from the climate station closest to Dungeness NWR, located in Sequim. An average of 8.12 inches, or roughly 50 percent of the annual precipitation, at this station occurs during late fall and winter in the months of November, December, January, and February. By comparison, the summer months of June, July, and August receive an average of 2.11 inches, a scant 13 percent of the annual precipitation. Additionally, the rate of rainfall within the rain shadow differs from other areas on the Olympic Peninsula. This area frequently receives drizzle or light rain while other localities are experiencing light to moderate rainfall (WRCC 2011a). On average, 5 days per year experience more than 0.50 inch of precipitation and 1 day greater than 1.00 inch (WRCC 2011e). Snow events are infrequent. However, snowfall increases with distance from water and rise in terrain. Consequently, the snow is a major source of water for the Dean Creek system, which passes through the Dawley Unit. Precipitation data for Sequim are summarized in Table 3-3.

**Table 3-3. Precipitation Summary near Dungeness NWR (WRCC 2011e)**

Precipitation (inches)	Sequim 2 E Oct. 1980 – Dec. 2010
Average Annual Precipitation	16.02
Average Annual Snowfall	1.5
Average Monthly Snowfall Range (winter)	0.2 to 0.9
Highest Annual Snowfall	13.7 (1989)
Highest Monthly Snowfall	25.0 (Dec. 1996)
Wettest Year on Record	20.51 (1997)
Driest Year on Record	11.35 (1994)
Wettest Season on Record	9.18 (winter 1997)
Driest Season on Record	0.41 (summer 2003)

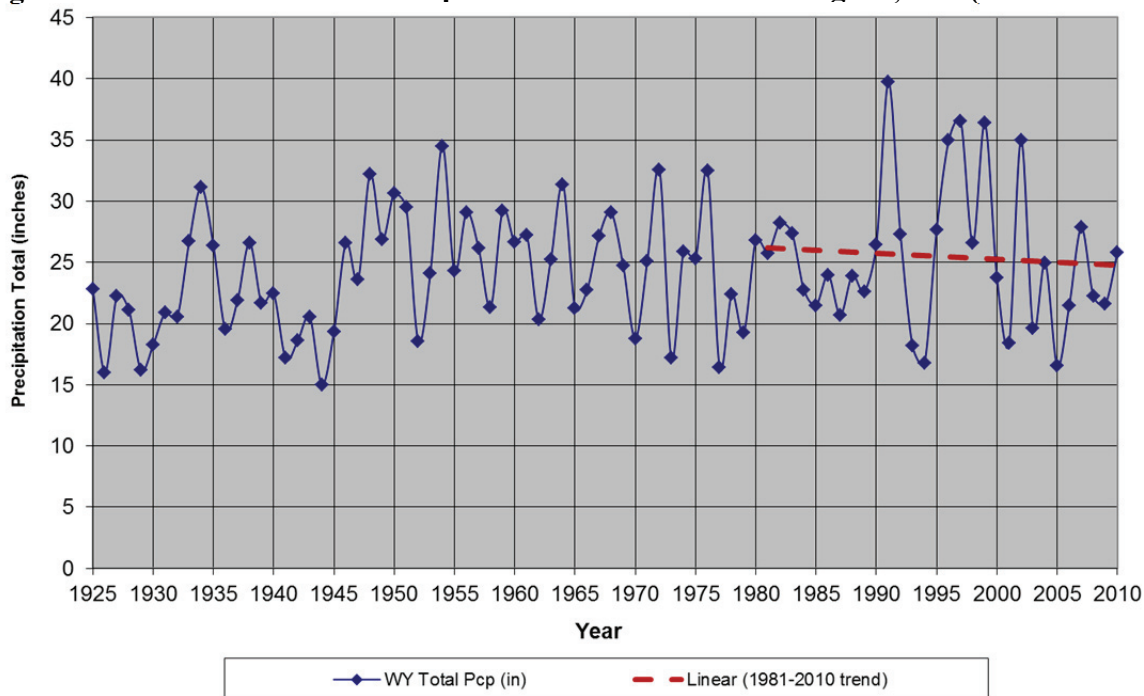
Longer-term precipitation trends in the Pacific Northwest are more variable than temperature and vary with the period of record analyzed (Mote et al. 2005). The Pacific Northwest experiences wide precipitation variability based on geography and seasonal and year-to-year variability (Salathé et al. 2010). Looking at the period 1920 to 2000, total annual precipitation has increased almost everywhere in the region, though not in a uniform fashion. Most of that increase occurred during the first part of the record with decreases more recently (Mote et al. 2005).

Precipitation trends from the Port Angeles USHCN observation station shows the average yearly precipitation change has decreased more than 5% over the past 30 years, with more striking decreases in the winter and increases in the summer (Table 3-4 and Figure 3-5).

**Table 3-4. Seasonal Precipitation Trends, 1981-2010 (USHCN 2012)**

<b>Port Angeles, WA, United States Historical Climatology Network Observation Station</b>	
Monthly Precipitation	30-year Change % from 1981 Value
Winter (Dec-Feb)	-17.1%
Spring (March-May)	14.3%
Summer (Jun-Aug)	-4.1%
Fall (Sept-Nov)	-1.6%

**Figure 3-5. Water Year Total Precipitation 1925-2010 at Port Angeles, WA (USHCN 2012)**



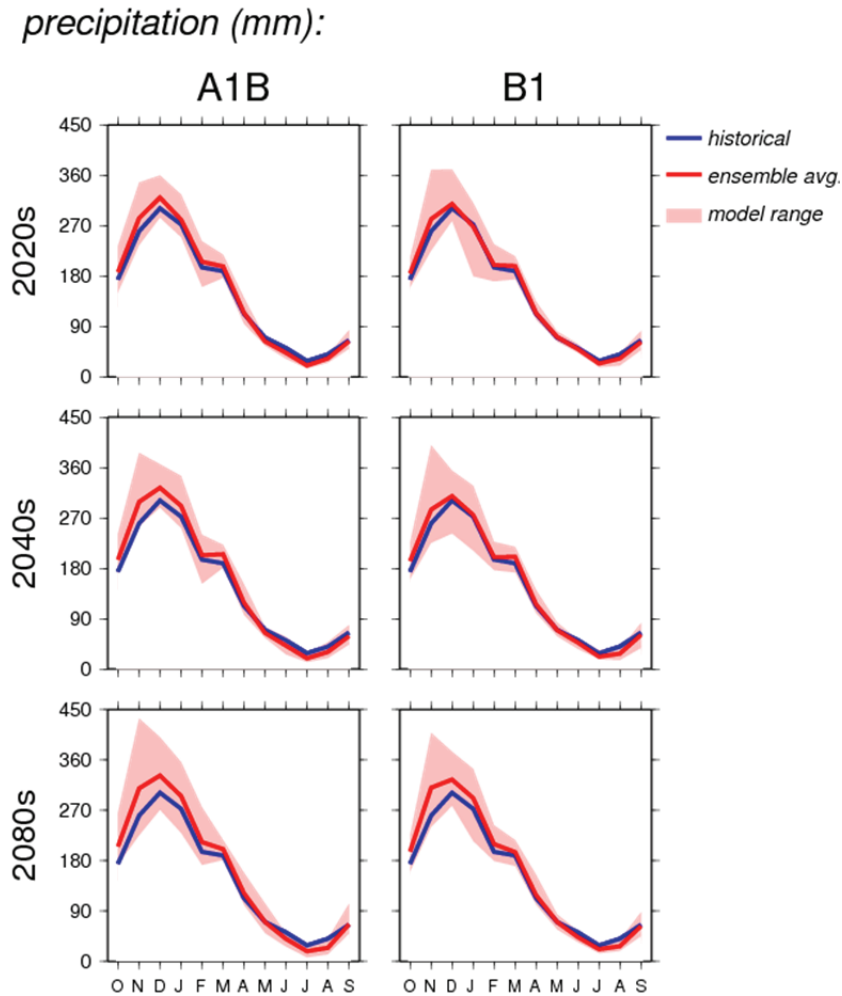
**Future Trends**

On a global scale, warmer temperatures are predicted to lead to a more vigorous hydrologic cycle, translating to more severe droughts and/or floods (IPCC 1996). Observations of Pacific Northwest precipitation trends through the 20th century indicate a region-wide increase of 14% for the period 1930-1995. Sub-regional trends ranged from 13% to 38% (Mote 2003). However, these trends are not statistically significant and depend on the time frame analyzed. Thus, decadal variability has dominated annual precipitation trends. Cool season precipitation variability, though, has increased (Hamlet and Lettenmaier 2007).

Using data derived from the statistical downscaling of 20 global climate models, projected changes in annual precipitation within the Pacific Northwest throughout the 21st century, averaged over all models, are small (+1% to +2%) though individual models produce changes of as much as -10% or +20% by the 2080s. Some models project an enhanced seasonal cycle with changes toward wetter autumns and winters and drier summers (Mote and Salathé 2010). However, even small changes in seasonal precipitation could have impacts on streamflow flooding, summer water demand, drought stress, and forest fire frequency. Additionally, researchers have consistently found that regional climate model simulations yield an increase in the measures of extreme precipitation. This finding suggests that extreme precipitation changes are more related to increased moisture availability in a

warmer climate than to increases in climate-mean precipitation (Leung et al. 2004, Salathé et al. 2010). Salathé et al. (2010) project increased extreme precipitation events in the State of Washington, with stronger increases in the northwestern portion of the state. The fraction of precipitation falling on days with precipitation exceeding the 20th century 95th percentile is projected to increase throughout the state. It is important to note that the one conclusion shared by researchers is that there is greater uncertainty in precipitation projections than that of temperature predictions and models (Leung and Qian 2003, CIG 2004, Salathé et al. 2010). Figure 3-6 shows these modeled, downscaled precipitation projections for the Dungeness-Elwha watershed (HUC 17110020) (Hamlet et al. 2010).

**Figure 3-6. Projected Precipitation Changes for the Dungeness-Elwha Watershed under Two Emission Scenarios (Hamlet et al. 2010)**



Note: A1B is a higher emission scenario than B1. Current rates are higher than both A1B and B1.

### 3.1.4 Wind

During the spring and summer, the semipermanent low-pressure cell over the North Pacific Ocean becomes weak and moves north beyond the Aleutian Islands. Meanwhile, a high-pressure area spreads over the North Pacific Ocean. Air circulates in a clockwise direction around the high-pressure cell bringing prevailing westerly and northwesterly winds. This seasonal flow is comparatively dry, cool, and stable (WRCC 2011a).

In the fall and winter, the high-pressure cell weakens and moves southward while the Aleutian low-pressure cell intensifies and migrates southward as well. It reaches its maximum intensity in midwinter. Wind direction switches to primarily southwesterly or westerly prevailing winds. The air mass over the ocean is moist and near the temperature of the water. As it moves inland, it cools and condenses, bringing the beginning of the wet season (WRCC 2011a).

Wind data collected hourly from an automated station located 14.5 miles west of the Dungeness NWR at the William R. Fairchild International Airport in Port Angeles, have been used to draw generalizations about wind activity in/on the Refuge (Table 3-5). Average wind speeds have been calculated on hourly data collected from 1996 to 2006. The highest average wind speeds occurred during the summer months of June and July. The calmest months were during the fall months of October and November.

Prevailing wind direction, defined as the direction with the highest percent of frequency, was calculated from hourly data during 1996 to 2006. Westerly winds occur from March through October, switching to southwesterly winds in November, and then to west-southwest during January, and southwest winds in February.

**Table 3-5. Wind Data Summary for Port Angeles (WRCC 2011f)**

	<b>Port Angeles</b>
Prevailing Wind Direction	W
Average Annual Wind Speed	5.2 mph
Average Monthly Wind Speed Range	4.2 (Jan., Oct., Nov.) – 6.6 (Jun., Jul.) mph

The open waters of the Strait of Juan de Fuca periodically allow very strong winds to develop, particularly during midlatitude cyclone events (Reed 1980). Wantz and Sinclair (1981) published estimates of extreme winds in the Northwest. They estimate that speeds within the vicinity of Dungeness NWR sustained for an average of one minute and recurring on average every two years are as high as 50 mph, while fifty-year events would produce winds of approximately 68 mph. Peak gusts would be about 32% higher.

As a rule, tornadoes are infrequent in Washington and generally small in the northwestern part of the United States. The National Climatic Data Center maintains a database that provides information on the incidence of tornadoes reported in each county in the United States. This database reports that 107 tornadoes were reported in Washington from 1950 to 2011. No tornadoes have ever been reported in Clallam County (NCDC 2011).

### **3.1.5 Climate Cycles in the Pacific Northwest**

Two climate cycles have major influences on the climate and hydrologic cycles in the Pacific Northwest: the El Niño/Southern Oscillation (ENSO) and the Pacific Decadal Oscillation (PDO). In El Niño years, average sea surface temperatures in the central and eastern equatorial Pacific Ocean are warmer than average and easterly trade winds in the tropical Pacific are weakened. A La Niña is characterized by the opposite – cooler than average sea surface temperatures and stronger than normal easterly trade winds. These changes in the wind and ocean circulation can have global impacts to weather events. The ENSO influence on Pacific Northwest climate is strongest from October to March. During an El Niño event, the winters tend to be warmer and drier than average. La Niña winters tend to be cooler and wetter than average. Each ENSO phase typically lasts 6 to 18

months and the shift between the two conditions takes about four years (CIG 2011, Conlan and Service 2000).

Like ENSO, the PDO is characterized by changes in sea surface temperature, sea level pressure, and wind patterns. The PDO is described as being in one of two phases: warm and cool. During a warm phase, sea surface temperatures near the equator and along the coast of North America are warmer while in the central north Pacific they are cooler. During a cool phase, the patterns are opposite. Within the Pacific Northwest, warm phase PDO winters tend to be warmer and drier than average while cool phase PDO winters tend to be cooler and wetter than average. A single warm or cool PDO phase lasts 20-30 years. The triggering cause of the PDO phase shift is not understood.

The potential for temperature and precipitation extremes increases when ENSO and PDO are in the same phases and thereby reinforce each other. When ENSO and PDO are in opposite phases, their opposite effects on temperature and precipitation can cancel each other out, but not in all cases and not always in the same direction (CIG 2011).

### **Future Trends**

Based on the evidence of the history of ENSO and PDO events, it is likely that these cycles will continue to occur far into the future. However, the potential influence of anthropogenic climate change on ENSO and PDO is unknown because more information is needed by the experts.

## **3.2 Hydrology**

### **3.2.1 Refuge Hydrology**

The circulation of Salish Sea region, which includes the Straits of Georgia, Juan de Fuca, and Puget Sound, is driven by tidal currents, the surface outflow of freshwater from river systems, and the deep inflow of saltwater from the ocean. The two major fresh water sources affecting the Refuge, the Dungeness River and Dean Creek, originate from the Olympic Mountains.

The headwaters of the Dungeness River begin in the steep alpine watershed of Olympic National Park. The Dungeness River and its tributaries drain about 200 square miles (322 square kilometers) and contain over 546 miles (879 kilometers) of river (Thomas et al. 1999). The Dungeness River flows generally north for about 32 miles, crossing the broad alluvial fan of the Sequim-Dungeness peninsula and into Dungeness Bay. The Dungeness and Graveyard spits separate Dungeness Bay and Harbor from the Strait of Juan de Fuca.

Dungeness Spit is a narrow, high-energy spit which extends approximately 5 miles northeasterly into the Strait of Juan de Fuca. Graveyard Spit is a broader, sheltered spit which extends south 1.4 miles from and in the lee of Dungeness Spit at a point about 3 miles out, creating a narrow channel between its southern terminus and the mainland. Graveyard Spit separates Dungeness Bay into two parts: the outer Bay and the inner Bay. The inner portion of Dungeness Bay, also known as Dungeness Harbor, has a surface area of 1.8 square miles or 1,151.5 acres (Rensel 2003).

Larger amounts of snow fall in the upper part of the Dungeness River drainage basin. This snow, along with glacier ice, is a major source of water to the Dungeness River system (BOR 2002). The river is a bimodal flow river, showing two peaks over the course of the year: a smaller peak associated with winter storm flows and a larger peak associated with snowmelt and runoff in the late

spring and early summer (EDPU 2005). According to the Dungeness-Quilcene Water Resources Management Plan (Jamestown S'Klallam Tribe 1994), "there is relatively little storage in the upper watershed, so that current-year precipitation directly controls runoff... and the rain shadow location exacerbates the late-summer low flow." Where the river empties into Dungeness Bay, the river flow situation is even more complex due to irrigation diversion and hydraulic continuity between the river and the shallow aquifer (Simonds and Sinclair 2002).

Groundwater is recharged primarily by precipitation, the Dungeness River and irrigation water. Recharge from irrigation ditch leakage may be predominating over precipitation recharge in some areas of the lower Dungeness watershed. Flow is generally south to north, following the slope of the land with the exception of some confined aquifers where vertical movement up or down is attributed to an artesian effect.

Dean Creek is an intermittent stream draining about one square mile. The creek drains the east side of Burnt Hill and the northwest side of Lookout Hill, flowing behind the 7 Cedars Casino into the southwest corner of Sequim Bay. A short (0.25 mile) reach of the creek runs through the Dawley Unit beginning at river mile 0.6 from Sequim Bay. The headwaters of Dean Creek begin at an elevation of 690 feet, approximately four miles from its mouth. The creek is in a degraded condition, with culverts in various locations, and incidents of severe flooding (EDPU 2005).

Tidal salt marshes are found on both the northern and southern ends of Graveyard Spit. Barrier lagoons and mudflats are located within the Refuge in the interior of both spits. Refuge mudflats are also east of Graveyard Spit in Dungeness Bay. Small (< 0.10 acre) seasonal freshwater wetlands are located within the Dungeness and Dawley units. For more information on Refuge wetlands, see Chapter 4.

A historic tidal lagoon and marsh was located at the base of Dungeness Spit. Today, dikes or old roadbeds, possible remnants of the old railroad grade or wharf, alter the hydrology of this tidal lagoon.

### **3.2.2 Tides and Salinity**

The nearest National Ocean Survey tidal benchmarks to Dungeness NWR are located in Port Angeles, approximately 13 miles west, and Port Townsend, approximately 18 miles east. Additionally, soundings collected in Dungeness Bay bathymetry in 2000 were analyzed and modeled to provide local tidal datums (Rensel 2003). Tidal benchmark information for Port Angeles and Port Townsend for the 1983-2001 period and tidal datums calculated for inner Dungeness Bay are summarized in Table 3-6. Historic records of tides and water levels from the Port Angeles and Port Townsend tide stations are summarized in Table 3-7. Data for each station include mean ranges, diurnal ranges, and the minimum and maximum water levels on record where available. The mean range is the difference in height between the mean high water and the mean low water. The diurnal range is the difference between the mean higher high water and the mean lower low water of each tidal day.

**Table 3-6. Tidal Benchmark Summary for Port Angeles and Port Townsend, Washington and Tidal Datum Summary for Inner Dungeness Bay (NOAA 2011a, NOAA 2011b, Rensel 2003)**

Station Information	Port Angeles Sta. ID 9444090	Port Townsend Sta. ID 9444900	Inner Dungeness Bay (05/2000)
Mean Higher High Water (MHHW) (ft)	7.07	8.52	7.55
Mean High Water (MHW) (ft)	6.52	7.84	6.89
Mean Tide Level (MTL) (ft)	4.23	5.17	N/A
Mean Sea Level (MSL) (ft)	4.25	4.99	4.59
Mean Low Water (MLW) (ft)	1.93	2.50	2.30
North American Vertical Datum 1988 (NAVD88)	0.43	N/A	N/A
Mean Lower Low Water (MLLW)	0.00	0.00	0.00

**Table 3-7. Historic Tidal Data Summary for Port Angeles and Port Townsend, Washington (NOAA 2011c, NOAA 2011d)**

Station Information	Port Angeles Sta. ID 9444090	Port Townsend Sta. ID 9444900
Mean Range (ft)	4.60	5.34
Diurnal Range (ft)	7.06	8.52
Mean Tide Level (MTL) (ft)	4.23	5.17
Minimum Water Level (ft below MLLW)	-4.83 (06/13/1982)	-4.22 (12/12/1985)
Maximum Water Level (ft above MHHW)	10.52 (01/02/2003)	11.73 (12/10/1993)

Tides are semidiurnal in Dungeness Bay, with higher high low, lower high and lower low tides generally occurring within a 24 hour 50 minute period. The mean tidal range, which relates to flushing ability, within the inner bay is approximately 4.4 feet. The water residence time in the inner bay averages about 40 hours. Details on tidal circulation can be found in Appendix A of *Dungeness Bay Bathymetry, Circulation and Fecal Coliform Studies* (Rensel 2003).

It is anticipated that the warming of Washington's temperate climate will contribute to fundamental changes along the coast, including but not limited to shifts in the timing and intensity of coastal storms, changes in precipitation and the delivery of freshwater inputs, sea level rise, and increased inundation of the shallow tidal basins. Regional coastal climate change may also result in changes in the intensity and timing of coastal upwelling, shifts in temperatures and dissolved oxygen concentrations, and alteration of the carbonate chemistry of nearshore waters. The combination of these changes will alter chemical concentrations in tidally influenced areas (Ruggiero et al. 2010). Dungeness Bay may experience changes in the salinity regime in response to changes in precipitation and snow melt in the watershed (resulting in changes in freshwater inflows) and increased intrusion of seawater associated with rising sea levels. However, the effect of climate change on salinity will vary with location and the magnitude of the relative sea level rise rate.

### 3.2.3 Sea Level Rise

Sea level rise on the Washington coast is the result of three major forces: global mean sea level rise driven by the melting of land-based ice, local dynamical sea level rise driven by changes in wind

which pushes coastal waters toward or away from shore, and localized vertical land movements driven primarily by tectonic forces (Mote et al. 2008, McKay et al. 2011). Mean sea level is defined as the average sea level over a 19-year period, about which other fluctuations (e.g., tides, storm surges, etc.) occur (Smerling et al. 2005). Global mean sea level rise has been in the range of 1.3 to 2.3 millimeters per year (0.05 to 0.09 inch/year) between 1961 and 2003 (IPCC 2007a). But since 1993 the rate has increased about 50% above the 20th century rise rate to 3 millimeters/year (0.12 inch/year) (Bromirski et al. 2011), and the latest global satellite sea level observations have risen to 3.19 millimeters/year (0.13 inch/year) (NASA 2012). This acceleration is primarily the result of ice field and glacier melt-off (McKay et al. 2011). For example, the total global ice mass lost from Greenland, Antarctica and Earth's glaciers and ice caps between 2003 and 2010 was about 4.3 trillion tons (1,000 cubic miles), adding about 0.5 inch (12 millimeters) to global sea level in a seven year period (Jacob et al. 2012).

In addition, vertical land movements are occurring as the North American plate and the off-shore Juan de Fuca plate collide. Uplift, which may offset local sea level rise, occurs along the Washington coast, while subsidence occurs off-shore. For example, while tide gauge data in Seattle reflect the global trend of about 2 millimeters/year (0.08 inch/year), at Neah Bay at the western end of the Strait of Juan de Fuca, relative sea level is falling because rapid uplift of the Olympic Peninsula outpaces global sea level rise. An interpolation of regional uplift rates based on an analysis of 29 tide gauges and 113 pairs of level lines provides an estimate of approximately 1-1.5 millimeters/year (0.04-0.06 inch/year) uplift in the vicinity of Dungeness NWR (Verdonck 2006).

Based on monthly mean sea level data from 1975 to 2006, the mean sea level trend at Port Angeles is 0.19 millimeter/year (0.007 inch/year) with a 95% confidence interval of  $\pm 1.39$  millimeters/year ( $\pm 0.054$  inch/year), which is equivalent to a change of approximately +0.06 feet per century (NOAA 2011e). Data for Port Townsend were recorded from 1972 to 2006 and indicates a mean sea level trend 1.98 millimeters/year (0.077 inch/year) with a 95% confidence interval of  $\pm 1.15$  millimeters/year ( $\pm 0.045$  inch/year), which is equivalent to a change of +0.65 feet per century (NOAA 2011e).

### **Future Trends**

The IPCC Special Report on Emissions Scenarios (SRES) forecasted that global sea level would increase by approximately 12 inches (30 centimeters) to 39 inches (100 centimeters) by 2100 (IPCC 2001). However, more recent analyses (Chen et al. 2006, Monaghan et al. 2006) indicate that the eustatic rise in sea levels is progressing more rapidly than was previously assumed, perhaps due to the dynamic changes in ice flow omitted within the IPCC report's calculations. Vermeer and Rahmstorf (2009) suggest that, taking into account possible model error, a feasible range by 2100 might be 30 inches (75 centimeters) to 75 inches (190 centimeters) (Vermeer and Rahmstorf 2009).

Tebaldi et al. (2012) show that even seemingly low increases in sea level will have impacts in the short term when storm surges are taken into account. An analysis of historic data is combined with future projections of sea level rise to estimate future return periods for what today are considered 50-year and 100-year events. This magnifies sea level rise by a factor of five, on average, and dramatically increases the occurrence, or return periods, of storm surge events.

Rising sea levels may result in tidal marsh submergence (Moorhead and Brinson 1995) and habitat migration as salt marshes transgress landward and replace tidal freshwater and brackish marsh (Park et al. 1991). Changes in tidal marsh area and habitat type in response to sea level rise were modeled using the Sea Level Affecting Marshes Model (SLAMM 6), which accounts for the dominant

processes involved in wetland conversion and shoreline modifications during long-term sea level rise (Park et al. 1989, Clough et al. 2010, Clough and Larson 2010). Within SLAMM, there are five primary processes that affect wetland fate under different scenarios of sea level rise: inundation, erosion, overwash, saturation, and accretion. There are currently several active projects involving the use of SLAMM 6 to estimate the impacts of sea level rise on the coasts and salt marshes of the Pacific Northwest (e.g., Glick et al. 2007).

For Dungeness NWR, SLAMM 6 was run using mean and maximum estimates from scenario A1B from the SRES. Under the A1B scenario, the IPCC AR4 (IPCC 2007a) suggests a likely range of 0.21 to 0.48 meter (0.7 to 1.6 feet) of sea level rise by 2090-2099 “excluding future rapid dynamical changes in ice flow.” The A1B-mean scenario that was run as a part of this project falls near the middle of this estimated range, predicting 0.40 meter of global sea level rise by 2100. The A1B-maximum scenario predicts 0.69 meter of sea level rise by 2100. To allow for flexibility when interpreting the results, SLAMM was also run assuming 1 meter, 1.5 meters, and 2 meters (3.3 feet, 4.9 feet, and 6.6 feet) of eustatic sea level rise by the year 2100. Pfeffer et al. (2008) suggests that 2 meters (6.6 feet) by 2100 is at the upper end of plausible scenarios due to physical limitations on glaciological conditions. Model results through 2025 for Dungeness NWR are presented in Table 3-8 (Clough and Larson 2010). All model results are subject to uncertainty due to limitations in input data, incomplete knowledge about factors that control the behavior of the system being modeled, and simplifications of the system.

**Table 3-8. Predicted Change in Acreage of Land Categories at Dungeness NWR by 2025 Given SLAMM-modeled Scenarios of Sea Level Rise (Clough and Larson 2010)**

	Initial Condition	Sea Level Rise Scenarios*				
		A1B Mean (0.39 m by 2100)	A1B Maximum (0.69 m by 2100)	1 m by 2100	1.5 m by 2100	2 m by 2100
Open Ocean	249.8	257.3	296.4	411.9	469.9	476.8
Tidal Flat	620.9	611.2	606.5	598.7	584.2	568.4
Undeveloped Dry Land	394.7	306.1	299.3	287.6	271.1	258.0
Estuarine Beach	145.5	146.6	146.5	146.4	146.2	145.9
Ocean Beach	130.1	204.0	170.1	62.9	16.7	19.6
Brackish Marsh	25.0	25.0	25.0	25.0	25.0	25.0
Salt Marsh	18.6	18.9	19.0	19.0	19.2	19.5
Swamp	7.8	7.8	7.8	7.8	7.8	7.8
Developed Dry Land	6.8	6.8	6.8	6.8	6.8	6.8
Estuarine Open Water	2.5	12.3	17.0	25.1	39.9	55.9
Inland Open Water	0.7	0.7	0.7	0.7	0.7	0.7
Transitional Salt Marsh	0.0	5.7	7.3	10.5	15.0	18.1

\* 0.39 m = 1.3 feet, 0.69 m = 2.3 feet, 1 m = 3.3 feet, 1.5 m = 4.9 feet, and 2 m = 6.6 feet.

### 3.3 Ocean Chemistry

The ocean will eventually absorb most carbon dioxide released into the atmosphere as a result of the burning of fossil fuels and other sources. Current rates of carbon dioxide emissions are causing and an increase in the acidity of ocean surface waters and a decrease the saturation of calcium carbonate ( $\text{CaCO}_3$ ), a compound necessary for most marine organisms' development of shells and skeletons (Hönisch et al. 2012). Oceanic absorption of  $\text{CO}_2$  from fossil fuels may result in larger acidification changes over the next several centuries than any inferred from the geological record of the past 300 million years (with the possible exception of those resulting from rare, extreme events such as meteor impacts). In the past 300 million years, three analogous ocean acidification events have been identified and these events coincided with mass extinctions of marine organisms, however it should be noted that warming and corresponding oxygen depletion co-occurred during these events and contributed to the extinctions (Hönisch et al. 2012).

Virtually every major biological function of marine organisms has been shown to respond to acidification changes in seawater, including photosynthesis, respiration rate, growth rates, calcification rates, reproduction, and recruitment. Much of the attention has focused on carbonate-based animals and plants which form the foundation of our marine ecosystems. An increase in ocean acidity has been shown to impact shell-forming marine organisms from plankton to benthic mollusks, echinoderms, and corals (Doney et al. 2009). Many calcifying species exhibit reduced calcification and growth rates in laboratory experiments under high- $\text{CO}_2$  conditions. Ocean acidification also causes an increase in carbon fixation rates in some photosynthetic organisms (both calcifying and noncalcifying) (Doney et al. 2009, Smith and Baker 2008, OCBP 2008). These potential impacts to the marine food web may obviously negatively affect Refuge resources such as seabirds, shorebirds, and salmonids. Localized acidification rates within Dungeness Bay have not been evaluated.

### 3.4 Topography and Bathymetry

The topography of Dungeness and Graveyard spits is largely flat, with most areas below 15.0 feet North American Vertical Datum 1988 (NAVD88) in elevation (PSLC 2001). The spits are comprised of series of shallow dune ridges and troughs with accumulation of drift logs on the surface. The narrowest portion of Dungeness Spit measures only approximately 50 feet wide, and intermittent overwash events have been documented during and after large storms.

Tidelands of the second class located within Dungeness Bay and surrounding the spits are managed by the Service under a perpetual easement with the Washington Department of Natural Resources and include mud and sand flats exposed only at low tide. The average depth of the inner Dungeness Bay is 8.3 feet (Rensel 2003). Shallower areas occur at the north part of the inner bay, while the deepest areas are located just west of Graveyard Spit and northwest of Cline Spit. A comparison of bathymetry, between 1967 and 2000, shows that the bay became shallower during that time period (Rensel 2003).

Bluffs at the base of Dungeness Spit are approximately 90-100 feet high while bluffs west of the spit rise to about 130 feet. The forested areas within the Dungeness Unit are primarily between 90 to 130 feet (NAVD88).

The northeastern portion of the Dawley Unit fronts Sequim Bay. The topography then generally slopes upward from northeast to southwest. Dean Creek flows from south to north through the

southeastern corner of the unit. Maximum elevations within the Dawley Unit are approximately 650 feet (NAVD88).

## **3.5 Geology and Geomorphology**

### **3.5.1 Regional Geologic Context**

Dungeness NWR is located on the northeast coast of the Olympic Peninsula along the Strait of Juan de Fuca. South of the Refuge, the jagged peaks of the Olympic Mountains loom over a deep, forested labyrinth of canyons. The Olympic Mountains originated from subduction of the denser Juan de Fuca Plate of oceanic crust underneath the North American Plate of continental crust in an area known as the Cascadia Subduction Zone. This subduction caused the superficial rocks of the descending oceanic plate (an accretionary wedge) to be progressively scraped off and accreted to the continental margin (Tabor and Cady 1978). Due to the subduction and the accretionary wedge, there are two lithologic assemblages that can be found on the Olympic Peninsula: the peripheral and core rocks.

The peripheral rocks, part of the Coast Range Terrane, consist of oceanic crust that was accreted onto the continent by either the collision of an intra-Pacific seamount province or by backarc or forearc rifting at the North American plate margin (Wells et al. 1984, Clowes et al. 1978, and Babcock et al. 1992 cited in Brandon et al. 1998). The Coast Range Terrane is composed of a basal unit called the Crescent Formation and an overlying Eocene to lower Miocene marine clastic sequence known informally as the Peripheral sequence (Brandon et al. 1998). The Crescent Formation consists of thick basalt flows such as pillow lava that are cut by dikes and interbedded with pelagic limestone and mudstone (Brandon et al. 1998). On the present day Olympic Peninsula, the peripheral rocks form a horseshoe shaped belt that rings the core rocks on the northern, eastern, and southern sides of the peninsula.

The core rocks are known as the Olympic Subduction Complex and they encompass mélangé scraped off the subducting Juan de Fuca plate and thrust, or underplated, on the bottom of the continental crust. This stacking of successive scrapes thus continually thickens and raises the older, top surface. As the subduction process at the Cascadia Subduction Zone continues, uplift occurs. At the same time, erosion eats away at the oldest, top sediments. Rocks of the Olympic Subduction Complex were first thrust above sea level about 12 million years ago and accretion and uplift presently outpace erosion in some parts of the range and so the Olympic Mountains are still rising, with the fastest rates occurring within the western part (Thackray and Pazzaglia 1994, Brandon et al. 1998).

Extensive glaciation over time has greatly shaped the Olympic Peninsula. The latest glaciation, the Fraser, lasted from about 23,000 to 11,000 years ago. The last major advance during the Fraser Glaciation occurred during the Vashon Stade, roughly 14,000 to 17,000 years ago (Hellwig 2010). At its maximum during the Vashon Stade, the margin of the Cordilleran ice sheet that influences the Olympic Peninsula originated in British Columbia, moved down through Georgia Strait on a base of advance outwash sands and gravels, proceeded south through the Puget Lowland to below the present city of Olympia (the Puget Lobe), and extended out the Strait of Juan de Fuca to beyond Cape Flattery (the Juan de Fuca Lobe).

The upper parts of watersheds draining into the Strait of Juan de Fuca were carved by alpine glaciers, which formed in the high mountain peaks of the Olympic Range and moved downstream. As the ice sheet retreated, widespread glacial deposits (outwash, drift, and till) were left behind. The lower

watersheds were cut by glacial water outflows and formed gently sloping plains of glacial till and outwash. Since glaciation, landforms have been modified by mass wasting, surface erosion, and deposition.

### 3.5.2 Refuge Geology

Dungeness and Graveyard spits are elongate spits primarily composed of well-sorted sand, gravel, and cobble which originate from erosion of adjacent mainland bluffs, alongshore sediment transport (shore-drift), and from washover deposits where the spits are narrow enough for overwash processes (Schwartz et al. 1987). The feeder bluffs are typically composed of Holocene-Pleistocene undifferentiated surficial (clay, silt, sand, gravel, till, diamicton, and peat) and landslide deposits (clay, silt, sand, gravel, and larger blocks deposited by mass wasting) that are at the edge of Pleistocene glaciomarine drifts (Schasse 2003). Net shore-drift patterns at the Dungeness Spit are driven primarily by fetch exposure. Sediment eroded from the glacial bluffs to the west is transported to the east, around the end of Dungeness and then along the recurve of Graveyard Spit. On the mainland, shore-drift converges from the east and west upon Cline Spit (Schwartz et al. 1987).

Using a comparison of historic maps of Dungeness Spit from dating 1855, 1926, and 1979 in conjunction with field surveys conducted in 1985, Schwartz et al. (1987) measured an eastward growth of the spit of about 1,900 feet (575 meters) over a period of record of 130 years. This elongation of Dungeness Spit was confined to that portion of the spit east of the junction with Graveyard Spit, as both Graveyard Spit and the west end of Dungeness Spit have remained relatively unchanged since the 1855 land survey. The study found an average elongation rate of 14.4 feet/year (4.4 meters/year) for the spit which agreed closely with 14.8 feet/year (4.5 meters/year) calculated by Bortleson et al. (1980). The volumetric increase in Dungeness Spit was estimated at about 65,305,000 cubic yards (1,850,000 cubic meters) from 1855 to 1985.

At the Dawley Unit, a portion of the unit adjacent to Dean Creek is underlain by Crescent Formation (middle and lower Eocene) basalt and basalt breccia. The lower part of Dean Creek, as it passes through the Refuge, is underlain with Vashon Stade advance glacial outwash, which is comprised of stratified, well-sorted sand, gravel, lacustrine clay, and silt deposited by meltwater during the glacial advance. The remainder of the unit occurs on Vashon Stade glacial till, which consists of unstratified, poorly sorted clay, silt, sand, gravel, and boulders directly deposited by the glacier (Schasse and Logan 1998).

## 3.6 Soils

All soil types and descriptions are mapped and described in the Soil Survey of Clallam County, Washington (USDA 2012). The principal soil types at the base of Dungeness Spit are Dick loamy sand (0 to 15 percent slopes) and Hoypus gravelly sandy loam (0 to 15 percent slopes). The Dawley Unit is made up of several soil types: Hoypus gravelly sandy loam (0 to 15 percent slopes, 15 to 30 percent slopes, and 30 to 65 percent slopes), Dick loamy sand (0 to 15 percent slopes), and Clallam gravelly sandy loam (15 to 30 percent slopes).

Dick loamy sand and Hoypus gravelly sandy loam are very deep, somewhat excessively drained soils formed in glacial outwash and found on outwash terraces. Permeability of these soils is rapid with a low water capacity. Consequently, runoff is slow. The effective rooting depth for both soils is 60 inches or more. Below a mat of organic material, the surface layer of Dick loamy sand is grayish

brown and dark brown loamy sand about 3 inches thick. The next layer is brown sand about 19 inches thick. The upper 26 inches of the underlying material is light olive brown and yellowish brown, stratified sand to loamy sand, and the lower part to a depth of 60 inches or more is olive brown and dark yellowish brown, stratified gravelly sand to gravelly loamy sand. The surface of Hoypus gravelly sandy loam is typically covered with a mat of organic material 1 inch thick. The surface layer is very dark grayish brown gravelly sandy loam 3 inches thick. The upper 7 inches of the subsoil is dark brown gravelly sandy loam, and the lower 21 inches is dark yellowish brown very gravelly loamy sand. The upper 14 inches of the substratum is dark brown very gravelly sand, and the lower part to a depth of 60 inches or more is dark yellowish brown gravelly sand.

Clallam gravelly sandy loam is a moderately deep, moderately well drained soil formed in compact glacial till and found on hills. Permeability of this soil is moderate to the compact glacial till and very slow through it. Available water capacity is low. Runoff is medium, and the hazard of water erosion is slight. The effective rooting depth is 20 to 40 inches. Water is perched above the compact glacial till from January through April. Typically, the surface is covered with a mat of organic material 2.5 inches thick. The surface layer, where mixed to a depth of 6 inches, is dark brown gravelly sandy loam. The upper part of the subsoil is brown gravelly sandy loam about 4 inches thick, and the lower part is brown very gravelly sandy loam about 18 inches thick. Compact glacial till is at a depth of 28 inches. Depth to glacial till ranges from 20 to 40 inches.

## **3.7 Fire**

### **3.7.1 Presettlement Fire History**

Dungeness NWR is in the driest area in western Washington (please refer to the Precipitation section for further discussion). Consequently, prior to Euro-American settlement, the predominant vegetation on lowlands west of the Cascades, from the Willamette Valley of Oregon north to the Georgia Basin of southwest British Columbia, was a mosaic of grasslands, oak and conifer forests, savannas, and various types of wetlands (Chappell and Crawford 1997). These forests, savanna, grassland, and herbaceous bald ecosystems generally rely on fire to maintain their vegetative structure and species composition. In addition to lightning-caused fires, historical accounts have also established that Native Americans used prescribed burning to create habitat for game animals and to promote the growth of weaving materials and food (Agee 1993, Chappell et al. 2001). The historic frequency with which a given area burned depended directly upon the number of natural and human ignited fires. Other factors affecting fire frequency and fire intensity include plant community types, changes in topography (i.e., slope and aspect), varying fuel accumulations, and variation in seasonal precipitation. The advent of Euro-American settlement interrupted Native American land management practices and altered the natural fire regime by eliminating prescribed fires and suppression of natural fires.

The watershed of the Dungeness River has experienced repeated large, intense wildfires prehistorically as a result of a number of climatic patterns, including long-term temperature cycles, a rain shadow effect from the adjacent Olympic Mountains, jet stream patterns, and prevailing west-to-east winds (DAWACT 1995, BOR 2002). Large, intense, stand-replacement wildfires have swept across the watershed at intervals of approximately 200 years with surviving older trees generally restricted to higher elevations and along riparian corridors. Present data indicate that large, stand-replacing fires occurred in A.D. 1308, 1508, and 1701 in the Dungeness watershed (DAWACT

1995). The intervals between these fires were long enough to permit growth of a replacement stand and accumulation of both ground and ladder fuels within the forest (BOR 2002).

### **3.7.2 Postsettlement Fire History**

In the areas dominated by Douglas-fir, such as on the mainland portion of Dungeness NWR and the Dawley Unit, the natural fire regime was probably similar to that described by Agee (1993) in coastal Douglas-fir forests. The majority of fires in the region are human-caused and starts occur during the dry summer months. A large, human-caused fire occurred in 1890 in the foothills between Port Angeles and Sequim, smoldered over the winter, and flared up again in 1891. Although not as extensive as the prehistoric fires, the 1890-1891 fire burned large areas of the lower Dungeness watershed. Numerous smaller fires have also occurred in the watershed with significant ones reported in 1860, 1880, 1896, 1902, 1917, and 1925. Few fires have occurred in the watershed since 1930, largely as a result of improved fire prevention techniques and increased levels of summer precipitation (DAWACT 1995, BOR 2002).

All known fires at Dungeness NWR were human-caused. The 1969 Dungeness Annual Narrative related the investigation of a fire started on June 3, 1969 when U.S. Coast Guard personnel were burning their garbage dump behind the residence. High winds caused the fire to quickly spread into the dry grass and driftwood affecting a total of 17 acres. Driftwood logs tend to smolder for weeks after the initial burn. The 1971 Dungeness Annual Narrative reported a fire at the junction of the main spit and Graveyard Spit on June 27 and 28, of that year. The 1983 Dungeness NWR Fire Management Plan states that between 1980 and 1983, two small unwanted fires originated on the spit from Native American campfires. In June 1989, the Ravine Fire burned 0.1 acre near the eastern boundary of the mainland portion of the Refuge. In June 1999, the Dungeness Fire burned 1 acre on Dungeness Spit, and a month later, the Lighthouse Fire burned 50 acres at the extreme end of the spit. The latter fire burned around New Dungeness Light Station with no damage.

## **3.8 Environmental Contaminants**

### **3.8.1 Air Quality**

The air quality may be affected by various activities on and adjacent to the Refuge including: marine vessels, industrial facilities, automobiles, and other human caused activities such as outdoor burning, wood stoves, and operation of various vehicles and machines (e.g., gasoline powered equipment, motorboats). The Refuge staff uses various types of equipment and transportation methods to achieve the Refuge habitat conservation projects and research. Habitat improvement projects and monitoring activities may include the use of tractors, heavy equipment, and/or the operation of trucks, boats, or other transport. Refuge visitors generally drive their automobiles to visit the various units of the Refuge and others operate motor boats within Dungeness Bay to fish or access the lighthouse.

### **3.8.2 Water Quality**

A state is required to identify waters that do not meet that state's water quality standards under Section 303(d) of the Clean Water Act (CWA). These waters are considered "water quality limited" and placed on the state's 303(d) impaired waters list. Section 303(d) requires the state to develop Total Maximum Daily Loads (TMDLs) for impaired water bodies. TMDLs are the amount of each

pollutant a water body can receive and not exceed water quality standards. Water quality standards for Washington include beneficial uses, narrative and numeric water quality criteria, and antidegradation policies. The Washington Department of Ecology (WDOE) assesses water segments according to parameters including bacteria, bioassessment, contaminated sediments, dissolved oxygen, pH, total phosphorus in lakes, temperature, total dissolved gas, toxic substances, and turbidity.

Dungeness Bay was listed as impaired in the 2008 303(d) reporting cycle for the following parameters: fish habitat and fecal coliform bacteria. A TMDL for fecal coliform was established in 2004 to address elevated fecal coliform levels that were impairing water quality and shellfish harvest. The Dungeness River has been identified as a source for nutrient loading and elevated fecal coliform problems from agricultural and residential runoff. Fecal coliform bacterial contamination and nutrient loading from animal waste were found on both commercial and small farms with high livestock concentrations and poor management. Existing on-site sewage disposal systems continue to have the potential to contribute bacterial contamination and nutrients to both surface and groundwater due to soil conditions and inadequate maintenance. Terminating near the Dungeness River delta and in several locations along the shoreline of the southern side of Dungeness Bay are outfalls for approximately 97 miles of irrigation ditches that divert water from the Dungeness River to agricultural and residential lands. These ditches are also likely contributing to the elevated fecal coliform problems in Dungeness Bay. Within 10 miles of the Refuge, there are five additional major subdrainages within the Dungeness River area watershed. These include McDonnell, Siebert, Bagley, Cassalery, and Gierin Creeks. There are approximately 546 miles of streams and tributaries in the overall watershed as identified in the 1993 Dungeness River Area Watershed Management Plan. Similar agricultural/residential runoff issues are likely associated with these drainages and are likely contributing to the existing problems with elevated fecal coliform bacteria.

Because of the shallow depth to groundwater, the lack of a confining layer in many areas, and porous soils, groundwater in this area is highly susceptible to nonpoint chemical contamination. In 1990, wells sampled by Clallam County showed levels of nitrate, although generally well below the drinking water standard, were elevated in some areas, and it was concluded that this was an upward trend. The source or sources for this contaminant is likely attributable to failing septic systems, livestock waste and agricultural/residential fertilizer usage combined with the presence of highly permeable soils and nearly 100 miles of irrigation ditches.

### **3.8.3 Contaminants**

Considering the historical uses of Dungeness NWR and the Dawley Unit, environmental assessment studies have revealed some threats to the Refuge from contaminants. Some of these contaminant issues have already been addressed while others remain. Jurisdiction issues and other factors (e.g., exposure risks, funding, location, concentration, potential for movement of the hazard, and accessibility) influence the timing of remediation. Historical uses included military, navigational aids (lighthouse), residential, and commercial.

In 1857, prior to the establishment of the Refuge, a lighthouse station was constructed on the terminal end of Dungeness Spit. The United States Coast Guard (USCG) operated and maintained this facility in accordance with acceptable laws and practices during their years of operations. In 1974, the station was automated with aids to navigation. In March of 1994, the Coast Guard stationed the last keeper; then from March–September the USCG auxiliary staffed the lighthouse. September

of the same year the lease for the maintenance and operation of the historical structures transferred to the newly formed New Dungeness Chapter of the U.S. Lighthouse Society (Society). In 2003, the New Dungeness Chapter separated from the Society and formed the New Dungeness Light Station Association. The agreement between the USCG and the New Dungeness Light Station Association was modified to reflect this change and continues today. As identified in this CCP, in the event that the USCG declares the light station property excess to its needs, the Service will work with the USCG to bring the lighthouse and surrounding land into the Refuge System. As part of that transfer the Service would work with the USCG on any unresolved contaminants issues concerning the lighthouse site. Several known issues have already been identified by the USCG through their own investigations.

In 2003, the USCG contracted Tetra Tech, Inc., to conduct a Phase I environmental site assessment also called an Environmental Due Diligence Audit (EDDA). The purpose of this audit was to “evaluate a particular property for potential environmental contamination and liabilities from past or present use of the site” in this case the New Dungeness Light Station. There were two underground storage tanks, and one above ground tank, on site which were removed in 1998 and soils tested for total petroleum hydrocarbons. The results were below the Model Toxic Control Act concentrations and no remediation was required.

The USCG, in 2009, contracted with Engineering/Remediation Resource Group, Inc. to conduct a Phase II (EDDA). The objectives were to evaluate (1) the presence and concentrations of lead in paint on the interior and exterior walls of the present site structures; (2) the concentrations of lead in soil around structures compared with background concentrations; (3) the presence of asbestos-containing material (ACM) inside site structures; (4) the presence and concentrations of petroleum hydrocarbons quantified as total petroleum hydrocarbons (TPH) and metals in the cisterns at the station; (5) the presence and concentration of petroleum hydrocarbons quantified as TPH in soil associated with former aboveground storage tanks (ASTs), former underground storage tanks (USTs), former fuel lines, and the present and former oil houses; (6) the concentrations of metals in soil around the current and former paint locker compared with background concentrations; (7) the presence and concentrations of polychlorinated biphenyls (PCBs) in soil in the vicinity of the transformer building; (8) the presence of mercury in the lighthouse lantern room; and (9) background metal concentrations. Based on the findings and recommendations of this report further sampling and remediation actions would be required.

In 2006, the Dawley rental house, located on the south side of Highway 101 and the mobile home west of the main residence, were sampled for Asbestos Containing Material (ACM) and Lead Based Paint (LBP). The test results were negative for all samples. The beach house along Sequim Bay, northwest of the Dawley main residence, was also sampled for ACM and LBP with test results showing positive for ACM but negative for LBP. There was an UST removed, also in 2006, near the garage west of the Dawley main residence and a vehicle oil changing rack. From both of these there was soil contamination by petroleum products that required the removal of 26 tons of soil from the UST and 5 tons from the rack areas. The Mellus Cabin, located in the Dungeness Unit, was surveyed for Asbestos Containing Material (ACM) and Lead Based Paint (LBP) in 2010 by the USFWS Regional Environmental Compliance Coordinator. A small area of interior floor tile contains low levels of ACM and there was no detection for LBP on any surface. The Dawley main residence was also surveyed at the same time for ACM and LBP. These compounds were detected at various levels and locations in and around the structure. For any of the structures that tested positive for either survey, the Service would be required to contract remediation services prior to any construction work.

The Dawley forest unit contains several small dump sites of waste construction material, household appliances, and other miscellaneous debris. In 2006, the Service conducted a Phase I and Phase II Environmental Site Assessment of the Dawley Unit revealing ACM in two locations. These sites were cleaned up by a contractor in 2009. No other containments, other than personal structural debris remains on the site.

Creosote pilings and rogue creosote logs are also a source of contamination on the Refuge and removal is an on-going management activity. Contamination by creosote is a concern because of the presence of toxic polycyclic aromatic hydrocarbons (PAHs) that can leach into water and sediments where they accumulate and impact marine and nearshore organisms. Sometimes levels of these compounds can reach above Washington State Department of Ecology sediment quality standards (Holman et al. 2009). In 2006, the Service partnered with the Washington State Department of Natural Resources and removed 150 tons of these logs from the Refuge. In 2011, a survey was again conducted for creosote rogue logs accumulation levels and locations. The U.S. Navy removed creosote treated sight target pilings from Dungeness Bay in 2010 that were on Refuge tidelands.

The threat of oil spills is another concern that can affect all of the Refuge's nearshore habitats. According to the Washington State Department of Ecology over 41 million gallons of oil are delivered over sensitive waterways every day in Washington. The Strait of Juan de Fuca is one of the most critical maritime highways for both the United States and Canada. Tanker traffic alone through this area carries over 15 billion gallons of oil each year (WDOE 2009a). The Refuge works with many partners on oil spill prevention, preparedness, and response programs to protect the natural shoreline and marine resources.

**Document continues on next page.**